NAL PROPOSAL No. 0032

Correspondent: R. Hofstadter
Department of Physics
Stanford University
Stanford, Calif. 94305

FTS/Off-net: 415-841-5121
321-2300

TEST AND CALIBRATE A LARGE NaI(Tl) TANC DETECTOR AND TO MEASURE NEUTRAL HADRON TOTAL CROSS SECTIONS

R. Hofstadter, J. F. Crawford, E. B. Hughes, and R. F. Schilling

June, 1970

High Energy Physics Laboratory
W. W. Hansen Laboratories of Physics
Stanford University
Stanford, California 94305

and

Department of Physics
Stanford University
Stanford, California 94305

Preliminary Proposal

to the

NATIONAL ACCELERATOR LABORATORY

to

TEST AND CALIBRATE A LARGE NaI(Tl) TANC DETECTOR AND TO MEASURE NEUTRAL HADRON TOTAL CROSS SECTIONS

R. Hofstadter, J. F. Crawford, E. B. Hughes, and R. F. Schilling

June 1970

1. Introduction

A research program is presently under way at the High Energy Physics Laboratory (HEPL) to develop total absorption nuclear cascade (TANC) detectors for hadrons, both charged and uncharged, at super-high energies. Similar work, also at HEPL, has already demonstrated the very attractive characteristics possessed by total absorption shower counters (TASC) for electrons and γ-rays at high energies (see references 1 and 2 attached). These properties include 100% detection efficiency, large acceptance aperture, wide dynamic range, stability and simplicity of operation, fast time response and, not least, an excellent energy resolution. Monte Carlo calculations[3] lead us to expect that the properties of the TANC detector will parallel quite closely those of the TASC. At 100 GeV, for example, a TANC detector 7 nuclear absorption units in length and 3 absorption units in diameter should be able to define the energy of an incident hadron to 5% (FWHM). We propose to test at the National Accelerator Laboratory (NAL) a TANC detector which is already under construction at HEPL, and to apply this detector to physics experiments at NAL. This detector will be particularly suited to experiments demanding the detection and measurement of neutral hadrons.

To our knowledge no other laboratory is presently pursuing a TANC detector development program, and we know of no other instrument which has comparable potential at NAL energies. The most obvious alternative is the ionization calorimeter. This is basically a sampling device and is inevitably subject to the statistics of the sampling process. A reliable quantitative comparison between the TANC detector and the ionization calorimeter at NAL energies has not yet been made and will probably have to await the availability of the high energy test beams at NAL.

2. TANC Detector Development Program at HEPL

The aims of the current research program at HEPL include the following:

(a) The construction of a NaI(Tl) TANC detector 7 nuclear absorption units (~ 100 inches) in length and 2 absorption units (30 inches) in diameter. This detector will probably be available late in 1971 and will be initially tested at SLAC.

(b) A systematic study of the nuclear cascade process, both experimental and theoretical, in order to learn how best to construct a TANC detector.

(c) An investigation of the information to be gained from image intensifier photographs of the nuclear cascade in NaI(Tl). This should provide information on the incident hadron direction and possibly help to distinguish between different hadrons.

In addition, one of the participants in this proposed research program is currently engaged in a search for new scintillation materials which may be preferable to NaI(Tl) for TANC detectors. One possibility (see reference 4 attached) is thallium chloride, which is 1.9 times more dense than NaI(Tl) and should make possible TANC and TASC detectors correspondingly reduced in size. A small thallium chloride crystal, 3 inches in length and 3 inches in diameter, will soon be tested at HEPL.

5. Proposed Experimental Program at NAL

We propose, as Phase I of our experiment, to calibrate a large NaI(Tl) TANC detector at NAL up to the maximum energy possible using a momentum-analyzed proton beam. It will also be interesting and desirable to calibrate the detector in a pion beam.

The most obvious experimental applicationsof a calibrated TANC detector at NAL are the following:

(a) To survey the yields of γ-rays and neutral hadrons in secondary beams. Measurements of this type are presently being made at HEPL using TASC detectors, and preliminary studies have been made at SLAC.

(b) To measure neutron and K_L^o total cross sections as a function of hadron energy. We have already made such measurements at SLAC (see reference 5 attached), using time of flight (and not a TANC detector) to identify and to define the energy of the hadron. The time of flight technique will not be possible at NAL and the use of a fully developed TANC detector will be essential.

We propose, as Phase II of our experiment, to measure neutron and K_L^o total cross sections on hydrogen and deuterium as a function of hadron energy. These measurements will require substantially pure neutron and K_L^o beams, or the development of a technique for distinguishing between those two beam components. We would be interested in discussions with the NAL staff aimed at developing the best experimental approach, as we become more familiar both with the properties of the TANC detector itself and the characteristics of the neutral beams at NAL. It is also very likely during this process that we will identify other applications of both TANC and TASC detectors at NAL. Such applications might also emerge from our current research program in neutral beams at SLAC.

4. Experimental Arrangements

Phase I of the experiment can be conducted in check-out of test beams. It is difficult to estimate the total amount of beam time required but we would expect a need for several days, not necessarily in one continuous run.

We anticipate that the experimental arrangement and procedures for Phase II of the experiment will be quite similar to those described in reference 5 (with the substitution, of course, of a TANC detector as the primary hadron detector). Liquid hydrogen and deuterium targets approximately one meter in length will be required. The measurements will be made by the good geometry technique and the targets will be rotated in and out of the beam at frequent intervals. The total beam time employed will be quite short. Assuming a neutral hadron flux of 10^4/sec/10 GeV/c , measurements of an adequate statistical precision can be obtained in a matter of hours. In practice several days will probably be required for testing and several more for the systematic accumulation of satisfactory data. With the exception of sweeping magnets and beam collimators, all of the experimental apparatus can be supplied by HEPL.

REFERENCES

1. R. Hofstadter, E. B. Hughes, W. L. Lakin and I. Sick, Nature 221, 228 (1969).

2. E. B. Hughes, R. L. Ford, R. Hofstadter, L. H. O'Neill, and J. N. Otis, Proceedings of the 12th Scintillation and Semiconductor Counter Symposium, Washington, D.C., March 1970.

3. J. Ranft (to be published), Rutherford High Energy Laboratory preprint RPP/N 20.

4. R. Hofstadter, K. H. Rosette, M. R. Farukhi, G. R. Kramer, and C. Swinehart, Proceedings of the 12th Scintillation and Semiconductor Counter Symposium, Washington, D.C., March 1970.

5. W. L. Lakin, E. B. Hughes, L. Madansky, L. H. O'Neill, and J. N. Otis, Physics Letters (to be published).

Contract Nonr 225 (67) .N8022923
HEPL No. 579

(Reprinted from Nature, Vol. 221, No. 5177, pp. 228–230, January 18, 1969)

NaI(Tl) Total Absorption Detector for Electrons and γ-Rays at GeV Energies

by
R. HOFSTADTER
E. B. HUGHES
W. L. LAKIN
I. SICK
High Energy Physics Laboratory,
Stanford University, California

A total absorption NaI(Tl) detector can be used to define the energy of an incident electron, or γ-ray, to a precision of 1 to 2 per cent in the range of 4 to 14 GeV.

We wish to report a new and successful demonstration of the use of total absorption shower detectors for electrons and γ-rays in the GeV energy range. Such detectors have the following attractive properties: (a) 100 per cent detection efficiency; (b) good energy resolution; and (c) large dynamic range. Furthermore, there is virtually no upper limit to the energy detectable by this means because the size of the detector varies only logarithmically with the energy of the incident electron or γ-ray[1].

Total absorption γ-ray detectors[1], in which a large block of scintillator produces a light pulse proportional to the γ-ray energy, are frequently used in nuclear physics for γ-ray energies up to several tens of MeV. The absorbing material is often NaI(Tl), which has an excellent scintillation yield, a high density (3·67 g cm^{-3}) and a correspondingly small radiation length ($\sim$ 1 inch). The use of NaI(Tl) total absorption detectors at higher energies[2] has not become common, principally because of the required absorber size. Until the work reported here the properties of such detectors in the GeV range have remained totally unexplored. On the other hand, the absorber size needed at GeV energies can be deduced from both calculations[3] and measurements[4] of the electron–photon cascade, and NaI(Tl) crystals of the appropriate size are now available. We describe here the response of a suitably large NaI(Tl) total absorption detector to electrons, and therefore γ-rays, in the range 4–14 GeV.

The detector under discussion consists of six separate NaI(Tl) crystals, ranging in size from 11·5 inches to 13 inches in diameter and from 3·75 inches to 7 inches in thickness. Each crystal is sealed in a thin aluminium case and viewed radially by four RCA 8054 or 8055 photomultipliers. A photograph of one of the crystal assemblies is shown in Fig. 1. The six crystals are mounted coaxially to simulate one large crystal 27 inches (approximately 27 radiation lengths) thick. In the tests to be described, the crystals were placed in a momentum-analysed, negatively charged, 3° secondary beam at the Stanford Linear Accelerator Center. This beam was produced by bombarding a Be target with 16 GeV electrons and consisted predominantly of electrons over the whole range of secondary momenta. The monochromatic target image size of the beam was 0·75 inch × 0·75 inch at the position of the crystals and the horizontal momentum dispersion was 1·7 inch/per cent. A 4 foot steel collimator with a horizontal aperture of 0·5 inch was placed immediately in front of the crystals and allowed the beam particles to pass down the axis of the detector. The momentum spread in the accepted beam, essentially determined by the finite target size, was therefore $\sim$ 0·4 per cent.

The experimental apparatus is shown schematically in Fig. 2. Signals from the photomultipliers on each crystal were passively mixed and subsequently mixed with the signals from each of the other crystals to provide a single output pulse. The decay time of each photomultiplier pulse was $\sim$ 250 ns, characteristic of NaI(Tl), but the sum pulse was shaped during amplification to a symmetric pulse of $\sim$ 250 ns full width at half maximum. Although the signals from the crystals can easily be clipped to a half-width comparable with the rise time of the photomultipliers ($\sim$ 15 ns), no attempt was made to optimize the speed of the detector in the measurements to be described. Plastic scintillators S_1 (2·5 inches × 2·5 inches) and S_2 (0·5 inch × 0·5 inch) were used to define the incident beam and scintillators V_1 and V_2 to reject unwanted off-axis particles. Coincidences between S_1 and S_2 were used to open a 500 ns linear gate to pass the amplified analogue pulse from the NaI(Tl) crystals into a 256 channel pulse height analyser. The circuitry shown in Fig. 2 was used to prevent the gate opening more than once during each beam burst (1·5 μs) and to avoid recording pulse heights either (a) when two S_1S_2 coincidences occurred within 500 ns of each other, or (b) when an off-axis particle was detected by V_1 or V_2 either within 2 μs immediately preceding the coincidence or following the coincidence but within the 500 ns gate.

Fig. 3 shows the pulse height distribution observed

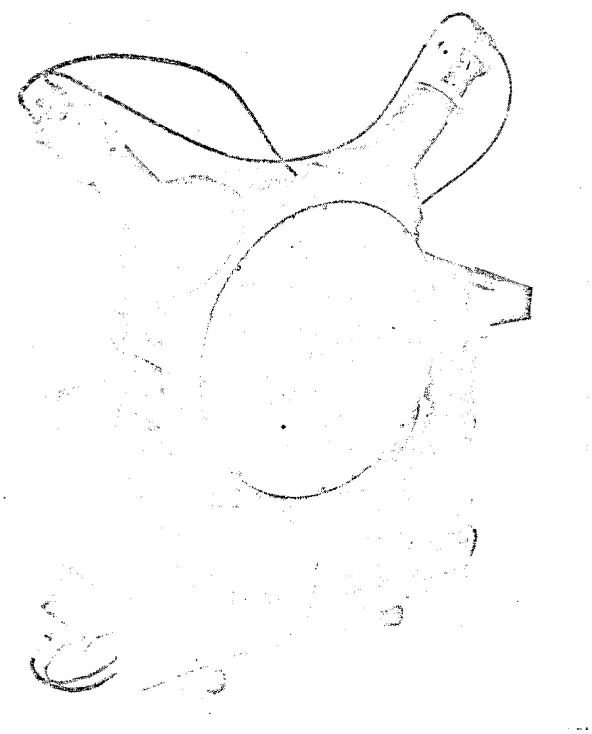

Fig. 1. A photograph of an NaI(Tl) crystal 13 inches in diameter and 7 inches thick, showing the crystal mounting. This crystal is viewed by four 5 inch RCA 8055 photomultipliers.

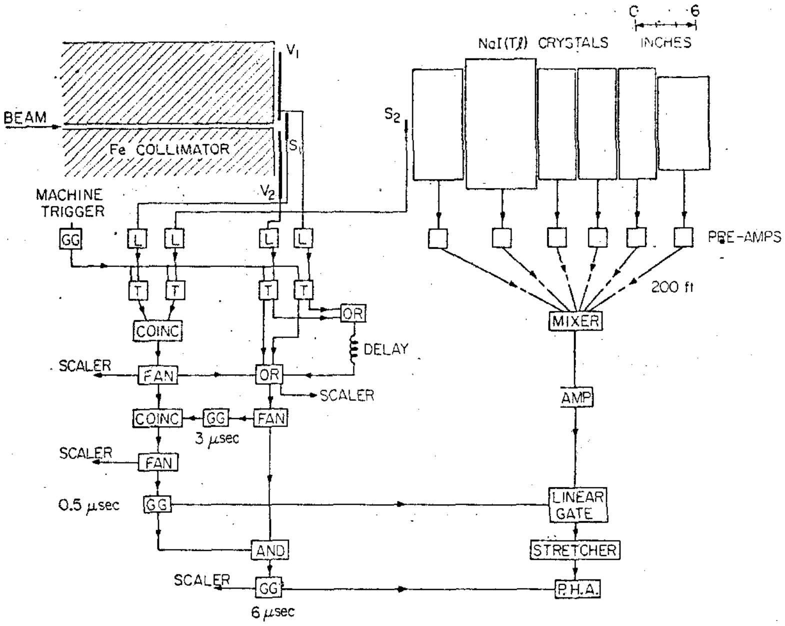

Fig. 2. Schematic diagram of the experimental apparatus and of the associated electronics.

when 8 GeV electrons are incident on the crystals. Fig. 4 shows the dependence of the resolution on electron energy in the range 4–14 GeV, and Fig. 5 shows the linearity of the relation between pulse height and electron energy. In preparing for these measurements the detector required one simple adjustment, the equalization of the gains of the six crystals relative to each other in order to compensate for the fluctuations in shower development. This was done by passing 8 GeV pions through each crystal in turn and normalizing the photomultiplier gains to the sharp edge in the Landau straggling distribution, corrected for the different crystal thicknesses. This method of equalization was checked by observing an electron peak and optimizing the photomultiplier gains to obtain the minimum peak width.

It is apparent from Fig. 4 that the observed resolution at all energies is clearly larger than that due to the spread in the beam momentum (~ 0.4 per cent). We consider the following additional sources of resolution.

(*a*) Photon statistics. Taking the number of photoelectrons produced at the photocathode to be ~ 5/keV, a 6 GeV electron will result in 3×10^7 photoelectrons. The statistical fluctuations in this number are extremely small (~ 0.04 per cent FWHM).

(*b*) Straggling in the crystal casings. The casing thickness in the plane perpendicular to the beam was 1/16 inch. This was artificially increased by inserting additional aluminium plates between adjacent crystals and measuring the resolution as a function of casing thickness. Extrapolation to zero thickness showed the contribution due to straggling to be $\lesssim 0.5$ per cent.

(*c*) Shower leakage from the crystal volume. The expected resolution due to leakage can be estimated from the Monte Carlo calculations of Völkel[3]. These calculations show that in the range 4 to 14 GeV a constant fraction, approximately 2·2 per cent, of the incident energy escapes from the crystal volume and that this escape is almost entirely radial. The radiation escaping is in the form of γ-rays and the spectrum of the escaping radiation, which peaks around 1 MeV, is essentially independent of the incident electron energy. These results imply a resolution due to leakage of 0·6 per cent (FWHM) at 4 GeV and 0·3 per cent at 12 GeV. These figures are not in good agreement with the measured values but do exhibit the observed improvement in the resolution with increasing energy.

(*d*) Photo-neutron production. Neutrons produced during electromagnetic showers initiated at GeV energies have been measured by Bathow *et al.*[5]. These results suggest that an average of 2·7 neutrons are produced during each 6 GeV shower and that this rate is dominated by photoproduction at the giant dipole resonance at 15 MeV γ-ray energy. If, as expected[6], the total track length for 15 MeV γ-rays varies linearly with the incident energy, the expected resolution due to neutron production is 1·2 per cent (FWHM) at 4 GeV and 0·7 per cent at 14 GeV. These estimates, which also predict an improvement in the resolution with increasing energy, must, however, be regarded as upper limits because each neutron has to traverse approximately one nuclear mean free path before it can escape from the crystal volume. A fraction of the energy expended in neutron production may therefore be returned to the crystal and the calculated resolution correspondingly improved. Nevertheless, until more is known about the production and reabsorption of neutrons in NaI(Tl), photo-neutron production must be regarded as a possible source of a significant part of the observed resolution.

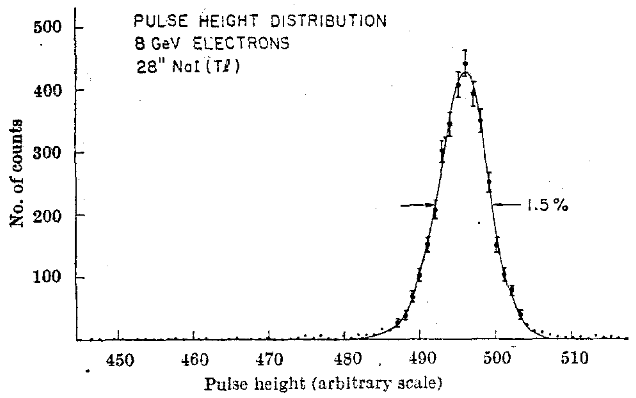

Fig. 3. The pulse height distribution observed when 8 GeV electrons are incident on the detector. The zero of the abscissa is offset to illustrate the peak shape. The curve is a Gaussian peak shape normalized to the height and width of the experimental distribution. This comparison is typical of the energy range 4 to 14 GeV.

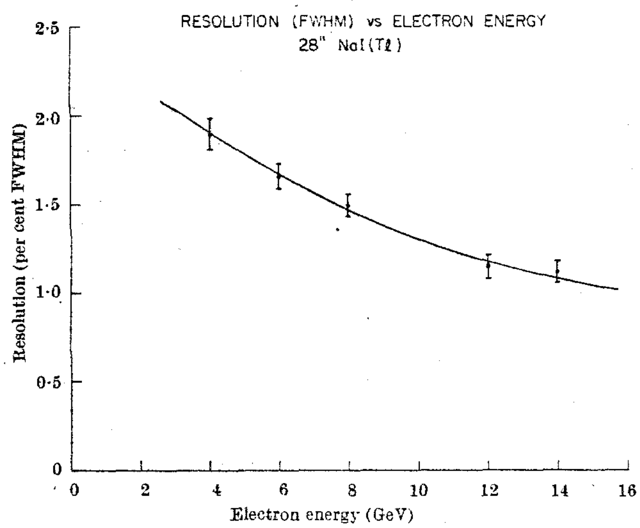

Fig. 4. The observed resolution (FWHM) versus electron energy.

We do not consider other sources of resolution, such as saturation effects in the photomultipliers during fluctuations in the shower development and variations in the light collection efficiency throughout the crystal volume. These effects are difficult to estimate but cannot be ignored at the level of resolution with which we are concerned. It is apparent, however, from tests performed by moving a ^{60}Co γ-ray source across one of the crystal faces, that the uniformity of the light collection efficiency is remarkably good. A change of less than 2 per cent was observed in the mean pulse height of a ^{60}Co peak (FWHM ~ 6 per cent) over 85 per cent of the crystal face. Nevertheless a reliable estimate of the limits to the resolution set by the light collection efficiency will require a careful study of the optical characteristics of these large crystal assemblies.

In summary, we find that a total absorption NaI(Tl) detector, approximately 11·5 inches in diameter and 27 inches long, can be used to define the energy of an incident electron, or γ-ray, to a precision of ~ 1–2 per cent in the range 4 to 14 GeV. We also find that this resolution is maintained over a circle of 7–8 inches diameter centred about the detector axis for electrons incident normal to the crystal face and that the resolution deteriorates by only a factor of two as the spectrometer length is reduced to 15 inches. We have not clearly identified the source of the observed resolution and cannot therefore define the limiting resolution which might eventually be achieved with this type of spectrometer. This conclusion depends, of course, on the reliability of the present Monte Carlo calculations on shower development, particularly at large depths in the absorber and at large distances from the shower axis and also at secondary photon energies as low as ~ 1 MeV. Finally, we note that the energy resolution already achieved by the NaI(Tl) detector in the GeV range is clearly superior to the alternative methods of total absorption which have been reported. These include lead-scintillator sandwich counters (21·6 per cent (FWHM) at 1 GeV and 7·6 per cent at 4 GeV)[7], and crystalline lead fluoride Cerenkov counters (7·5 per cent (FWHM) at 4 GeV and 5·5 per cent at 14 GeV)[8].

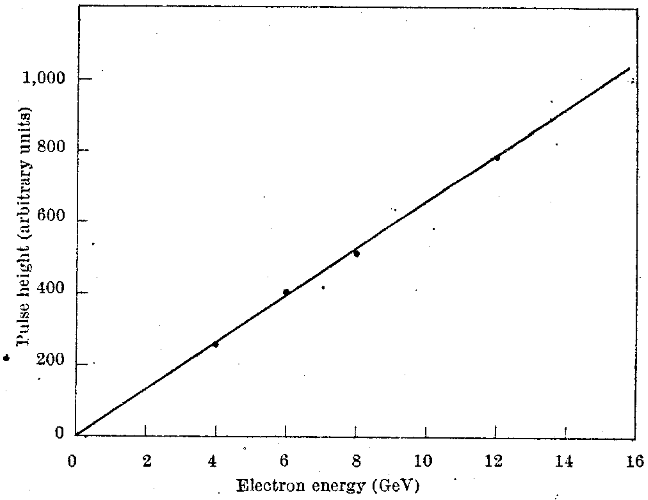

Fig. 5. The dependence of the mean pulse height on electron energy. No measurement is available at 14 GeV.

This work was supported in part by a US Office of Naval Research contract. We thank Dr Joseph J. Murray of the Stanford Linear Accelerator Center for making available the secondary beam at SLAC and, with Mr Roger A. Gearhart, for help in the use of this beam. We also thank Mr Douglas J. Norman for his help and the Harshaw Chemical Company for lending us some of the crystals used in the research.

Received December 30, 1968.

[1] Kantz, A., and Hofstadter, R., *Phys. Rev.*, **89**, 3 (1952); Kantz, A., and Hofstadter, R., *Nucleonics*, **12**, 36 (1954).

[2] Berezin, S., Hofstadter, R., and Yearian, M. R., *Bull. Amer. Phys. Soc.*, **7**, 620 (1962); Berezin, S., *Stanford University High Energy Physics Laboratory Report HEPL*-424; Berezin, S., thesis, Stanford Univ. (1967).

[3] Völkel, U., *DESY Report* 65/6 (July 1965); *DESY Report* 67/16 (May 1967).

[4] Crannell, C. J., *Phys. Rev.*, **161**, 310 (1967).

[5] Bathow, G., Freytag, E., and Tesch, K., *DESY Report* 66/13 (May 1966).

[6] Zerby, C. D., and Moran, H. S., *J. Appl. Phys.*, **34**, 2445 (1963).

[7] Heusch, C. A., *Proc. Intern. Conf. Electron-Photon Interactions*, Hamburg, II, 408 (1965).

[8] Dally, E. B., and Hofstadter, R., *Rev. Sci. Instrum.*, **39**, 658 (1968); *Stanford University High Energy Physics Laboratory Report HEPL*-531; Dally, E. B., and Hofstadter, R., *IEEE Trans.*, NS-15, 76 (1968); *Stanford University High Energy Physics Laboratory Report HEPL*-550.

Printed in Great Britain by Fisher, Knight & Co., Ltd., St. Albans.

IEEE TRANSACTIONS ON

NUCLEAR SCIENCE

JUNE 1970 VOLUME NS-17 NUMBER 3
Published Bimonthly

1970 TWELFTH SCINTILLATION AND SEMICONDUCTOR COUNTER SYMPOSIUM

Shoreham Hotel, Washington, D.C., March 11–13, 1970

Sponsored by

IEEE Nuclear Science Group, U.S. Atomic Energy Commission, and National Bureau of Standards

PROPERTIES OF A NaI(Tl) TOTAL ABSORPTION SPECTROMETER FOR ELECTRONS AND γ-RAYS AT GeV ENERGIES

E. B. Hughes, R. L. Ford, R. Hofstadter, L. H. O Neill† and J. N. Otis†
Department of Physics and High Energy Physics Laboratory
Stanford University, Stanford, California

In the past two years we have reported on the properties of large NaI(Tl) crystals as total absorption spectrometers for electrons and γ-rays in the range 0.1 to 14 GeV.[1,2] We have recently made similar measurements on a NaI(Tl) spectrometer which is both larger than any we have used before and assembled in a different way. In the following paragraphs we indicate the results of our initial tests.

The new spectrometer consists of three individually grown NaI(Tl) Harshaw crystals, optically cemented together, and mounted in a single aluminum casing. Each segment is 16" in diameter and 8" in length. The overall dimensions are therefore 16" in diameter and 24" in length. A schematic diagram of the spectrometer and experimental apparatus is shown in Figure 1. The crystal volume is viewed by five 5" RCA 8055 photomultipliers mounted on one end face, and the particle to be measured enters through a $13\frac{1}{4}$" diameter, 1/16" thick, aluminum window on the opposite end face. The signals from these five photomultipliers are summed to provide a single output pulse. Signals are also available from four 2" photomultipliers which are mounted in diametrically opposite positions symmetrically located with respect to two of the crystal segments. The purpose of these tubes is to permit some compensation to be made for the different intrinsic scintillation yields of the different crystal segments and for variations in the average light collection efficiency along the length of the spectrometer. Consideration was given during assembly to the choice of matched crystal segments and to the minimization of variations in the light collection efficiency, but residual amounts of both effects are present. This is apparent from Figure 2 which shows the results of a longitudinal survey made with collimated Co^{60} γ-rays. A similar survey was also made with 1 GeV electrons, incident perpendicular to the axis, in order to establish the validity of the result shown in Figure 2 along all trajectories parallel to the spectrometer axis.

Figure 3 shows the resolution observed as a function of electron energy, both for the main photomultipliers alone and for an optimum degree of compensation using the 2" photomultipliers. This resolution is available for electrons incident parallel to the axis and along all trajectories which enter the crystal not less than 2" from its edge. At all energies for which measurements were made, both at the High Energy Physics Laboratory and the Stanford Linear Accelerator Center, the momentum spread in the incident electron beam was less than 0.2% (FWHM). Figure 4 shows, for example, the resolution observed at 7.5 GeV as a function of a collimator aperture in a beam of known momentum dispersion. The action of the compensation photomultipliers is displayed in more detail in Figures 5 and 6. This method of compensation depends upon the selectivity of the response of the 2" photomultipliers to light directly emitted from the crystal segments to which they are coupled. This is clearly demonstrated in Figure 7 which shows the resolution obtained using the compensation tubes alone or in an optimum combination.

At this time we cannot point conclusively to the source of the residual line-width. Qualitatively, however, the properties of the spectrometer are such that a considerable fraction of the uncompensated resolution appears to be attributable to the different intrinsic scintillation yields and to a nonuniformity in light collection efficiency, as exhibited in Figure 2. Moreover we have no reason to expect that the present design provides the flexibility to compensate exactly for either of these two effects. We therefore think it probable that a significant improvement in resolution can be obtained with a spectrometer in which the above two deficiences are reduced still further.

While the performance of the present spectrometer is entirely adequate for many experiments in high energy physics, and is approaching results obtained with magnetic spectrometers, we are nevertheless continuing our efforts to develop a design which possesses the best possible resolution. Despite its limitations the resolution offered by the present detector for energies less than 1 GeV is a factor of two better than we have observed before. At higher energies the improvement factor decreases but is still a factor of 1.25 at 15 GeV.

It is worth noting that neither our experimental tests to date nor the Monte Carlo calculations we have made on the electron-photon cascade give any indication that fluctuations in shower leakage, corresponding to escaping gamma rays, make anything other than a minor contribution to the presently observed resolution. For example, at 1 GeV we have operated a NaI(Tl) crystal in the shape of an annulus in front of the present spectrometer. The dimensions of this crystal were the same as those of the individual segments in the spectrometer except for a 3" diameter hole about the axis. Its purpose was to detect back-scattered radiation, but no amount significantly affecting the resolution was observed. We have also made Monte Carlo calculations at 8 GeV to establish the expected resolution due to leakage from the sides and rear of the present spectrometer but find both components to be much smaller than the resolution so far observed.

Acknowledgements:

We gratefully acknowledge the cooperation and help of Mr. B. R. Chambers and Mr. L. G. Doster of the

High Energy Physics Laboratory, of Dr. J. J. Murray, Mr. R. A. Gearhart and Mr. F. T. Halbo of the Stanford Linear Accelerator Center, and of Mr. E. C. Stewart of the Harshaw Chemical Company.

References:

1. R. Hofstadter, E. B. Hughes, W. L. Lakin, and I. Sick, Nature, 221, 228-230 (January 1969).

2. E. B. Hughes, "Observations on the Total Absorption of Electrons and Pions in Matter at GeV Energies," NAS-NRC Publication (to be published); invited talk presented at the Washington meeting of the American Physical Society (April 1969).

---

*This work was supported in part by the U.S. Office of Naval Research Contract [NONR 225 (67)] and the National Science Foundation Grant GP-9498.

†National Science Foundation Predoctoral Fellow.

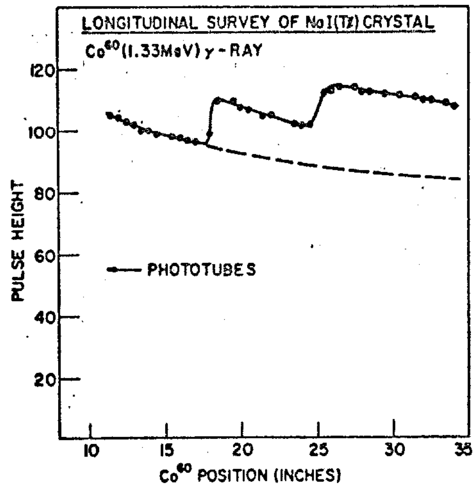

Fig. 2.

The results of a longitudinal survey of the spectrometer using a collimated Co^{60} γ-ray source. The individual crystal segments can be clearly seen. In the dashed curve the steps corresponding to the different scintillation yields of the three segments are removed and the remaining variation presumably represents the nonuniformity in the light collection efficiency.

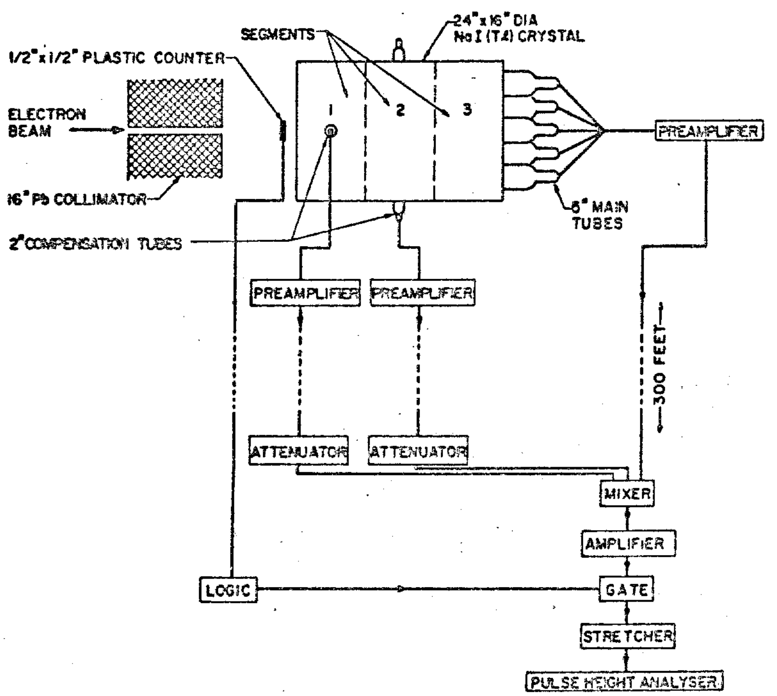

Fig. 1. A schematic diagram of the crystal spectrometer and experimental apparatus.

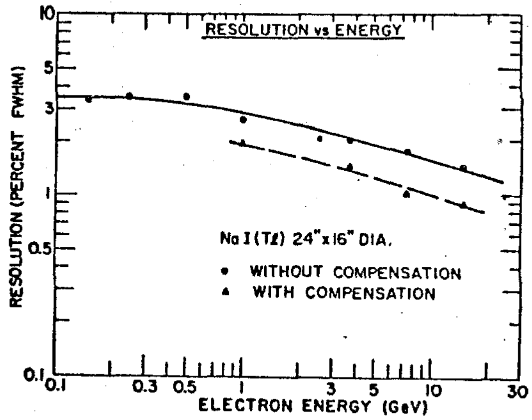

Fig. 3.

The observed resolution as a function of electron energy, with and without compensation.

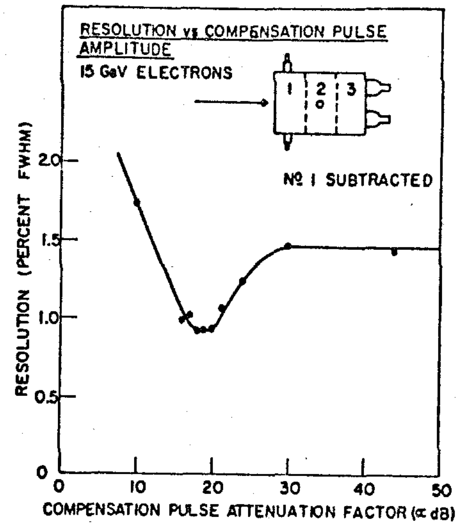

Fig. 5.

The electron resolution at 15 GeV as a function of the amount of compensation signal from segment 2 subtracted from the main signal.

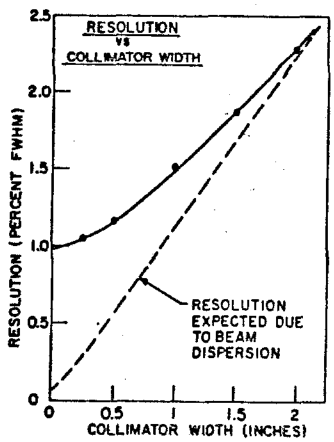

Fig. 4.

The electron resolution at 7.5 GeV as a function of collimator width in a beam of known momentum dispersion.

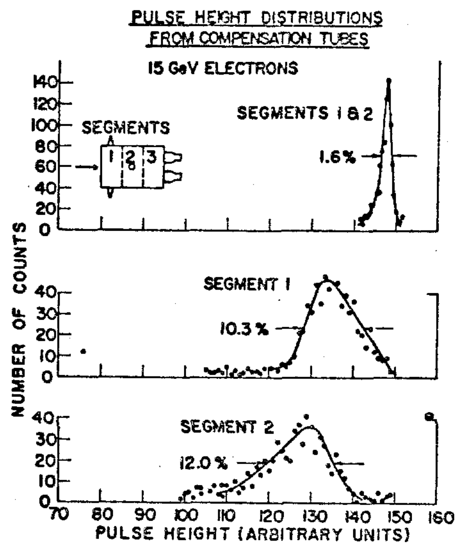

Fig. 7.

The pulse height distribution observed using the compensation photomultipliers alone or in combination. The correlation between the signals obtained from the photomultipliers on segments 1 and 2 is apparent.

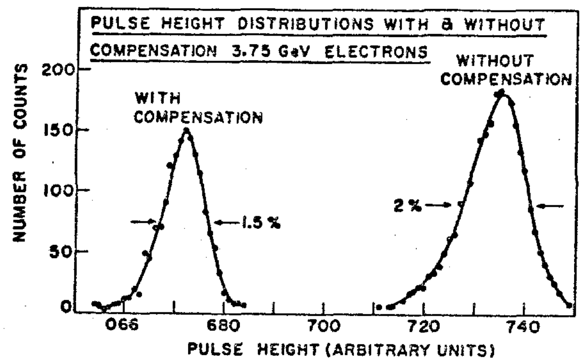

Fig. 6. The observed pulse height distribution with and without compensation. From the abscissa the amount of compensation signal subtracted can be seen.

IEEE TRANSACTIONS ON

NUCLEAR SCIENCE

JUNE 1970 VOLUME NS-17 NUMBER 3
Published Bimonthly

1970 TWELFTH SCINTILLATION AND SEMICONDUCTOR COUNTER SYMPOSIUM

Shoreham Hotel, Washington, D.C., March 11-13, 1970

Sponsored by

IEEE Nuclear Science Group, U.S. Atomic Energy Commission, and National Bureau of Standards

A HIGH Z SCINTILLATOR

K. H. Rosette, M. R. Farukhi, Gerald R. Kramer, and Carl Swinehart
Crystal & Electronic Products Department, The Harshaw Chemical Company, Division of Kewanee Oil Company, Solon, Ohio 44139

and

R. Hofstadter
Department of Physics, and High Energy Physics Laboratory
Stanford University, Stanford, California 94305

Summary

Thallium Chloride, activated with iodides, has been found to scintillate. Photopeaks for the Cs^{137} .662 Mev gamma energy have been obtained with several crystals, while many other TlCl crystals, prepared with different iodides of varying low concentration show smaller scintillation response.

Pulse height varies with the activators used. The consistently largest output to date is measured for TlCl(Be,I). A maximum pulse height of 2.5% relative to NaI(Tl) has been measured. The best resolution value is 42% at .662 Mev for Cs^{137}. The gamma ray excited luminescence agrees remarkably well with the low temperature intrinsic luminescence of TlCl at 4650 Å. A scintillation decay time of 0.2 microseconds is obtained.

Having good mechanical and thermal shock resistance, high density and the highest atomic number of any scintillator known to date, iodide activated TlCl promises to be an important new scintillator. The scintillation efficiency and decay time are sufficient for consideration in high energy counters and spectrometers.

Introduction

High energy detector size has become a crucial and challenging limitation. The recent development of the total absorption technique[1] poses the requirement of extremely large CsI(Tl) or NaI(Tl) crystal volumes. A higher Z scintillator would significantly reduce detector volume requirements and simplify related systems requirements such as structures and photomultiplier arrays.

At low and intermediate gamma ray energies, the larger photofraction of a high Z scintillator relative to a comparable size NaI(Tl) or CsI(Tl) detector may be advantageous even with a low light output and poor resolution, such as in counter applications. Optimistically, there is the possibility that a new high Z scintillator with low scintillation efficiency may be improved to yield good resolution at low energies for spectrometry.

We report here the discovery of scintillation in the high Z crystal, Thallium Chloride, activated with iodide containing compounds. The scintillation efficiency and decay time are sufficient for consideration in high energy counters. The performance at low energies is still limited by the low scintillation efficiency and resolution, but improvements can be expected with improved growth and activation techniques.

Undoped TlCl has received practical attention for optical applications, where its high index of refraction (2.400 at .436µ to 2.182 at 18.35µ) and transmission range from .40µ to 30µ are useful for lenses and prisms. TlCl is relatively insoluble and non-hygroscopic, unlike NaI(Tl) which must be hermetically canned. TlCl is soft and ductile and has good mechanical and thermal shock resistance.

Because of its high Z, density, excellent mechanical and chemical characteristics, TlCl is an exceptionally attractive scintillation host crystal.

Experimental Procedure

Over 150 crystals of undoped and doped TlCl were grown from the melt, starting with purified TlCl. Dopant compounds, or in several instances, cation elements and iodine, were thoroughly mixed with the TlCl powder prior to melting.

Nominally 1/2 inch diameter crystals were grown in pyrex or quartz test tubes in a controlled atmosphere Stockbarger[2] furnace. Both open tubes with an argon atmosphere and sealed ampoules were used. After growth, the crystals were annealed to room temperature at the rate of 5C° to 10C°/hr.

Because of the survey aspect of these initial dopings, the crystals generally did not represent the optimum in crystal perfection or homogeneity. Many were heavily overdoped as evidenced by cloudy and colored heel regions. However, in many cases, excellent, clear, water-white crystals were obtained.

In even the worst cases, we expect to have introduced our dopants at low concentration levels. At this preliminary point we can only refer to the "added" molar concentrations rather than actual concentrations. Our discussion of results will be confined to the effect of dopant composition rather than concentration.

Quantitative spectrographic analysis of several of the crystals did indicate the presence of the added iodine in the heel and cone regions. The systematic scintillation results with various dopant cations supports their presence in the crystals in addition to a few analyses. Having concluded our survey, we are presently investigating the actual dopant concentrations for optimum scintillation efficiency.

All ingots were directly tested for room temperature luminescence excited by Co^{60} and Cs^{137} gamma radiation to determine scintillator candidates. An RCA Quantacon C 31000D photomultiplier and Harshaw 2000B integrating picoammeter were used to detect ultra-low light levels.

Scintillation samples, typically 1/2 inch diameter and 1/2 inch long, were carefully prepared from crystals showing positive luminescence. Opposite faces were polished and cylindrical surfaces were roughened for diffuse reflection. The crystals were coupled to the photomultiplier tube with Dow Corning 20-057 silicone grease and covered with an aluminum can, coated with an Al_2O_3 reflector. The first stage GaP dynode of the photomultiplier provided increased sensitivity and resolution. A Harshaw NB-12 preamplifier and a Harshaw NA-16 pulse shaping amplifier with single differentiation of 6.4 microseconds were used with a Northern Scientific 512 multichannel analyzer.

Scintillation efficiency was measured as pulse height relative to a Harshaw Type D canned 1/2 inch diameter by 1 inch long NaI(Tl) crystal for the Cs^{137} .662 Mev line.

Of the crystals measured, 93 showed positive D.C. luminescence response and were tested for room temperature scintillation pulse response to Cs^{137} gamma radiation. 66 crystals showed pulses. Oscilloscope photographs were obtained which were helpful in determining weak pulses greater than .18% of NaI(Tl). 43 crystals had discernible Cs^{137} .662 Mev photopeaks and multichannel analyzer spectrum curves were used to obtain FWHM resolution values for the .662 Mev line.

Results

Fig. 1 summarizes the scintillation pulse height response for the crystals measured. The histogram shows the pulse height distribution for both iodide and non-iodide doped TlCl with various dopant cations. Table 1 identifies the dopant composition code used in Fig. 1.

We are unable to establish the existence of scintillation pulses less than 0.18% RPH because of the noise level. The first bar of Fig. 1 represents this questionable region. Several iodine doped samples appear in this region, but the histogram clearly shows the necessity of iodide activation for scintillation.

Furthermore we see the effect of the additional presence of certain cations. The largest pulse heights are consistently observed in (Be,I) doped TlCl, with a maximum of 2.5% RPH obtained. Likewise, (Cu,I) dopings show a consistent response. Large pulse heights are observed with Bi, Cd, Gd, B, NH_4 dopants added with TlI to TlCl.

We have several cases where the cation or secondary dopant is used with and without I. CuBr and CuCl doped samples respond in the noise whereas CuI doping results in significant scintillation. NH_4Cl doping is ineffective, but NH_4I doped samples show strong scintillation. Doping with $BeCl_2$ yields very weak pulses (a trace amount of iodine contamination is suspected), but (Be,I) doping results in the largest scintillation pulse heights observed. We note the weak pulse behavior of the dopant added as elemental iodine with a wide range of additional cation dopants. However, the use of $BeCl_2$ with elemental iodine results in large pulse heights.

In Fig. 2 we show the Cs^{137} FWHM resolution distribution for crystals whose photopeak spectrum could be obtained. All crystals represented contain iodide doping.

As expected from the pulse height data of Fig. 1, (Be,I) doping shows a consistently high resolution. The other strong scintillators of Fig. 1 show good resolution. These resolution measurements are also influenced by crystal homogeneity, scintillation activation uniformity and optical uniformity.

The best resolution of 42% for the Cs^{137} .662 Mev energy is shown in the spectrum in Fig. 3. A comparison of the ^{137} spectrum for a 1/2 inch by 1/2 inch (Be,I) doped TlCl crystal and a 1/2 inch by 1 inch NaI(Tl) crystal is made in Fig. 4. At the top is the NaI(Tl) full pulse height response. We then attenuate the NaI(Tl) response with a neutral density filter, attenuating the NaI(Tl) pulses to amplitudes comparable to that of the (Be,I) doped TlCl response shown at the bottom. Nearly identical photomultiplier and amplifier gains were used with weak scintillations for identical source geometry. We see the expected increase in the photofraction even though the NaI(Tl) crystal has twice the volume of the TlCl (Be,I) crystal.

Fig. 5 compares the linear attenuation coefficients of TlCl, NaI and CsI versus that of Pb. The large stopping power of TlCl is clearly evident and consistent with the spectra comparison of Fig. 4.

Preliminary measurements indicate an increase of pulse height at 77°K by a factor of between three and four. However a large increase in decay time is observed, approximately a factor of ten. In the case of the (Be,I) doped sample whose resolution is shown in Fig. 3, resolution and pulse height degradation is also observed upon cycling between room temperature and 77°K. The spectrum shown in Fig. 4 is the degraded response.

Typical decay times of 0.20 $\pm$ .02 microseconds are measured as indicated in Table 2, obtained from oscilloscope photographs of integrated pulses.

The room temperature luminescence spectrum for TlCl(Be,I) was measured for Co^{60} gamma excitation with a Bausch and Lomb Spectrometer, 500 mm focal length, 600 groove/mm grating blazed for 5000 Å. In order to obtain sufficient light output, three crystals were coupled for the measurement.

Curve I in Fig. 6 shows the room temperature luminescence of TlCl(Be,I) excited by Co^{60} gamma rays. Shown for comparison are the 364 mμ excited luminescence of pure TlCl at 77°K and 4°K reported by V. A. Sokolov.[3] There is excellent agreement in the peak emission wavelength at 4650 Å. This emission peak for pure TlCl has also been observed for x-ray excitation at low temperatures.[4]

Discussion of Results

The (Be,I) activation of TlCl appears to produce a modification of the intrinsic luminescence center normally operative at low temperatures. Pure TlCl, at temperatures above 170°K does not show the 4650 Å emission[5] which is consistent with the lack of room temperature scintillation in pure TlCl.

Recombination luminescence at a trapped hole after electron capture has been proposed for the low temperature intrinsic luminescence of TlCl.[3,4,6]

Our results indicate the necessity of iodide activation of TlCl for scintillation. Furthermore, enhancement of the scintillation efficiency results from particular secondary dopants, such as Be.

We believe vacancy modifications of Cl_2^- [7] and ICl^- [8] V centers in TlCl(Be,I) are responsible for the correlation of our luminescence results with the luminescence of pure TlCl at low temperatures. The enhancement effect of such cations as Be^{++} can be related to their production of Tl vacancies near I^- ions in doped TlCl.

The increased thermal stability of these complexed molecular ion centers,[7] the greater hole localization with I^- and favorable energy transfer between Tl^+ and I^- are significant in the scintillation process. Detailed investigations of these ideas are in progress at our laboratory.

Continuing High Z Program

Our research in Iodide Activated Thallium Chloride is presently directed toward obtaining:

(a) Larger volume TlCl scintillators of optical and activator uniformity necessary for good energy resolution at high energies.

(b) Greater scintillation efficiency to make useful low energy detectors where the ruggedness and large photofraction capability of TlCl are exceptionally attractive.

Large TlCl(Be,I) crystals are primarily a crystal growth program. Pure TlCl crystals of good optical quality have been grown to five inches in diameter by four inches long.[9] Doped large crystals pose additional growth complexities.

Scintillation efficiency is affected by crystal growth and doping techniques as they relate to crystal quality, luminescence centers, energy transport and quenching centers. Experimental and theoretical approaches are being pursued.

The upper limit for the scintillation efficiency may be small so that iodide activated TlCl may only be used in high energy physics applications. However, until the existence of such a limitation is proven, the attempts to increase the scintillation efficiency will be extensive.

Iodide activated TlCl thus promises to be a new important and interesting scintillator.

References

1. A NaI(Tl) Total Absorption Spectrometer for Electrons and γ-rays at *GeV Energies*, E. B. Hughes, R. C. Ford, R. Hofstadter, L. H. O'Neill and J. N. Otis, These Proceedings.
2. D. Stockbarger, J. Opt. Soc., Am. 39, 731 (1949).
3. V. A. Sokolov, Optika i Spektroskopiya, 21 (1), 98-100, 1966; Optics and Spectroscopy (USSR) 21, 53 July 1966.
4. A. D. Brothers and D. W. Lynch, Phys. Rev., 159, (3) 159 (1967).
5. V. A. Sokolov and N. A. Tolstoi, *Optika i Spektroskopiya*, 9, 421 (1960); Optics and Spectroscopy (USSR) 9, 219 (1960).
6. V. A. Sokolov and N. A. Tolstoi, Optika i Spektroskopiya, 18, 251 (1965); Optics and Spectroscopy (USSR) 18, 139 (1965).
7. W. Känzig, Phys. Chem. Solids, 17, 80 (1960).
8. Physics of Color Centers, Academic Press, New York and London, 1968, W. B. Fowler, Ed. p. 168.
9. Harshaw Chemical Co., Laboratory Report (1962), Private Communication.

Table I

Dopant Code to Fig. I

A.	NH_4I	a	$BeCl_2$
B.	BiI_3	b	LiF
C.	BI_3	c	CuCN
D.	TlI	d	Fe + I_2
E.	CdI_2	e	Mg + I_2
F.	GdI_3	f	$NiCl_2$ + I_2
G.	CuI	g	BN + I_2
H.	HgI_2	h	CuCl
I.	CsCl + NH_4I	i	CuBr
J.	LiCl + NH_4I	j	NH_4Cl
K.	$NiCl_2$ + NH_4I	k	$EuCl_2$
L.	AgI	l	Mn
M.	$CaCl_2$ + TlI	m	$MnCl_2$
N.	CsI	n	NaCl
O.	KI	o	$UO_2(NO_3)\cdot 6H_2O$
P.	RbI	p	YF_3
Q.	$SbCl_3$ + NH_4I	q	$YbCl_2$
R.	$CoCl_2$ + NH_4I	r	CuCl + I_2
S.	DyBr + NH_4I	s	$EuCl_2$ + I_2
T.	SiI_2	t	$ZnCl_2$ + I_2
U.	NaI	u	$MnCl_2$ + I_2
V.	HI	v	P + I_2
		w	I_2
		x	Ge + I_2
		y	Zn + I_2
		z	Al + I_2

Table 2.
Scintillation decay times for doped Thallium Chloride crystals

Crystal	Dopant	Decay Time (10^{-6} seconds)
138	CuI	.20 ± .02
126	BiI_3	.23 "
133	NH_4I	.18 "
82	Be,I	.21 "
124	Be,I	.21 "
122	Be,I	.23 "

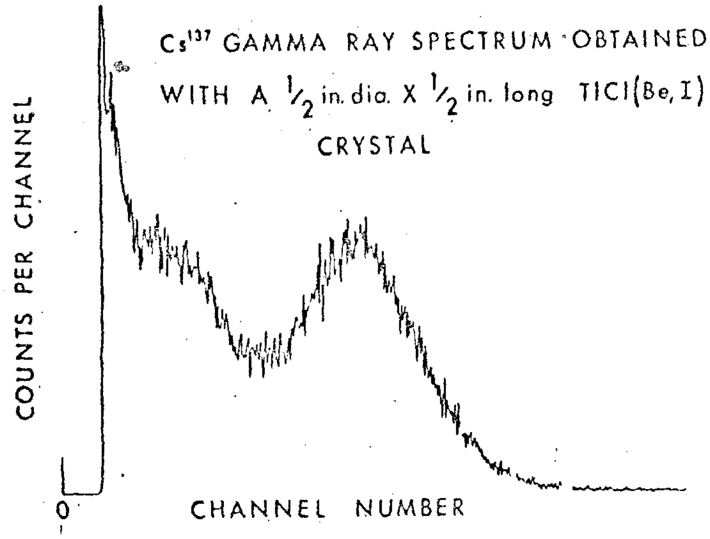

Fig. 3. Cs^{137} Gamma Ray Spectrum obtained with a TlCl (Be,I) crystal.

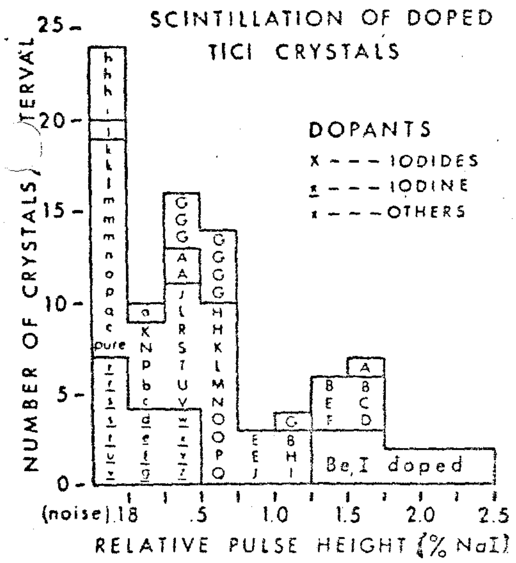

Fig. 1.
Scintillation pulse height distribution for doped Thallium Chloride crystals.

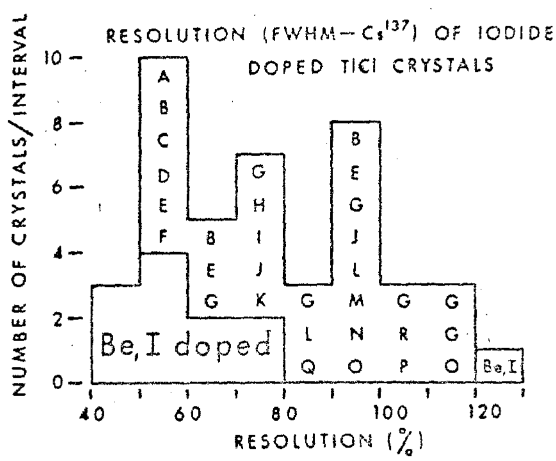

Fig. 2. Scintillation resolution distribution for doped Thallium Chloride crystals.

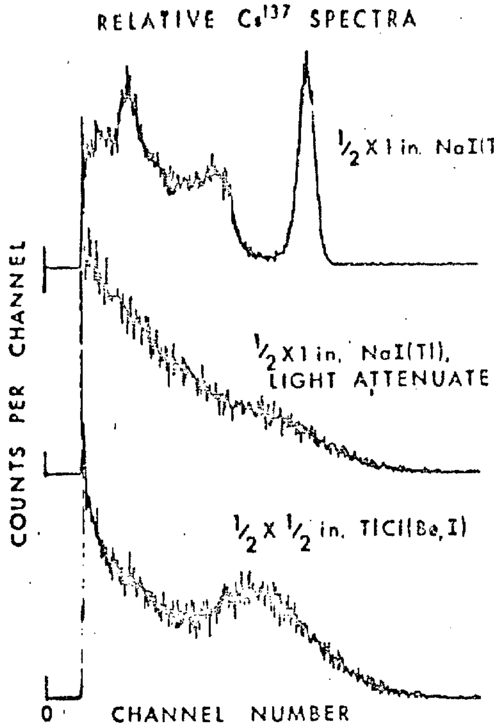

Fig. 4. Comparison of Cs^{137} Gamma Ray Spectra obtained with TlCl(Be,I) and NaI(Tl).

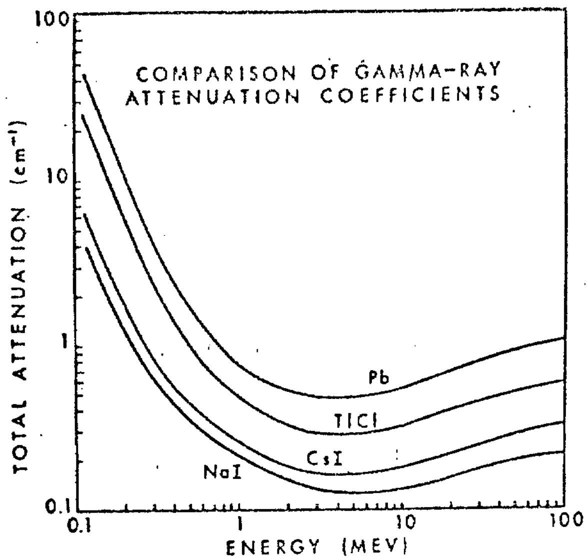

Fig. 5. Total linear attenuation coefficients of NaI(Tl), CsI(Tl), TlCl and Pb.

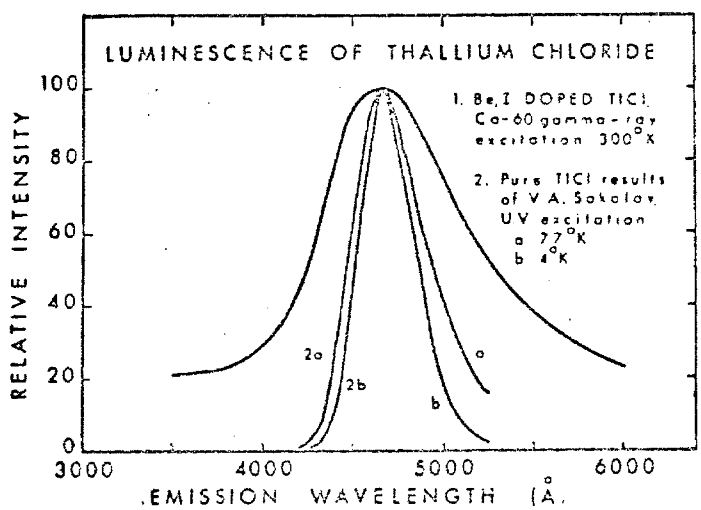

Fig. 6. Luminescence of TlCl (Be,I) and undoped TlCl.

(To be submitted to
Physics Letters)

HEPL 627
March 1970

MEASUREMENTS OF K_L^0 AND NEUTRON TOTAL CROSS SECTIONS ON NUCLEI AT GeV ENERGIES*

W. L. Lakin,† E. B. Hughes, L. H. O'Neill,‡ and J. N. Otis‡

High Energy Physics Laboratory

Stanford University

Stanford, California

and

L. Madansky§

Stanford Linear Accelerator Center

Stanford University, Stanford, California

MEASUREMENTS OF K_L^o AND NEUTRON TOTAL

CROSS SECTIONS ON NUCLEI AT GeV ENERGIES*

W. L. Lakin,† E. B. Hughes, L. H. O'Neill,‡ and J. N. Otis‡

High Energy Physics Laboratory
Stanford University
Stanford, California

and

L. Madansky§

Stanford Linear Accelerator Center
Stanford University, Stanford, California

ABSTRACT

Measurements of K_L^o and neutron total cross sections are reported for C, Al, Cu, and Pb at average momenta of 9.0 GeV/c for K_L^o and 3.8 GeV/c for neutrons. Comparison is made with the predictions of an optical model calculation.

MEASUREMENTS OF K_L^o AND NEUTRON TOTAL CROSS SECTIONS ON NUCLEI AT GeV ENERGIES*

W. L. Lakin,† E. B. Hughes, L. H. O'Neill,‡ and J. N. Otis‡

High Energy Physics Laboratory

Stanford University

Stanford, California

and

L. Madansky§

Stanford Linear Accelerator Center

Stanford University, Stanford, California

In this letter we report new measurements of the K_L^o and neutron total cross sections on four selected nuclei at GeV energies. We compare these measurements with the predictions of the optical model in the high energy approximation.(1) No previous measurements of K_L^o - nucleus total cross sections at GeV energies have been reported. Several measurements of neutron-nucleus total cross sections are available in the range 2.1 to 27 GeV/c,(2-7) but until recently these have not displayed a convincing consistency with one another. New measurements of neutron-nucleus total cross sections are clearly needed to clarify this situation.

The experiment was performed at the Stanford Linear Accelerator Center in a 3^o secondary neutral beam produced by 16 GeV electrons striking a beryllium target. A similar beam has been described by Brody, et al.[8] and after suitable filtration is expected to consist principally of K_L^o's and neutrons. In the present experiment the electrons struck the target in bursts of 0.3 nS duration at intervals of 50 nS, which permitted a time of flight measurement on each K_L^o or neutron detected. The neutral beam was collimated to an area 2.5 cm × 2.5 cm at a distance of 95 meters from the production target and, after passing through a sweeping magnet and clearing collimator, was incident on the detector located a further 51 meters downstream. This detector consisted of a sandwich of steel absorbers and plastic scintillators and is indicated schematically in Fig. 1. The small counters (T) provided a fast pulse which, together with a pulse derived from the time structure of the electron beam, was used in the time of flight measurement. Experience showed that this system provided a timing resolution of 0.7 nS (FWHM) which, over the flight path of 146 meters, corresponded to a maximum resolvable momentum of $\sim$ 8 GeV/c for kaons and $\sim$ 16 GeV/c for neutrons. The acceptance of the detector was restricted to an area 7.6 cm × 7.6 cm, centered about the beam axis, by a steel collimator located 2 meters upstream of the detector. The targets under investigation were inserted into the beam at a distance of 50 meters upstream of the detector at which point the detector subtended a half-angle of 0.8 mR. Total cross sections were measured in good geometry by rotating the targets in and out of the beam at about 1 minute intervals. This avoided the need for extreme stability in the beam monitors, two of which were used: a current integrator in the electron beam and a plastic scintillator in the secondary neutral beam.

The observed total cross sections are shown in Fig. 2 as a function of time of flight. The cross sections were measured both with and without an additional aluminum absorber inserted into the beam upstream of the target. The action of this absorber is to change the proportions of kaons and neutrons in each timing interval and to change, therefore, the apparent cross sections. It can be seen that the observed cross sections at both large and small flight times reach values which depend strongly neither on the flight time nor on the presence of the aluminum absorber. (Some variation of the cross section with flight time is expected even for pure K_L^o or neutron beams because of the energy dependence of the elementary hadron-nucleon cross sections. This variation should be more evident for short flight times due to the increasing insensitivity of the flight time to energy as the energy increases.) From this data we infer that, for flight times (relative to that for γ-rays) shorter than ~ 1.9 nS, the beam consists primarily of K_L^o's and that, for flight times longer than ~ 9.0 nS, the beam is essentially pure neutrons. These flight times correspond respectively to kaon momenta larger than 5.4 GeV/c and to neutron momenta smaller than 4.8 GeV/c. These conclusions are in essential agreement with expectations based on the kaon and neutron momentum distributions reported by Brody, et al.[8] However the rate of accumulation of events at short flight times indicates a kaon flux smaller than that reported by Brody, et al., by a factor of approximately 5.

We consider first the K_L^o total cross sections which can be obtained from the data in the flight time interval less than 1 nS. The cross sections were computed using each of the two monitors and the results differed by less than 0.1%. The background rate in the detector was measured and found to be negligible (~ 0.1%). There are two sources of systematic error, both of which can generate an admixture of neutrons in the accepted timing interval. First, slow neutrons produced in earlier pulses will be accepted if their flight times are integral multiples of 50 nS longer than those of the high energy kaons. This contribution can be reliably estimated from those events which occur several nanoseconds before the fast kaons which indicate an admixture of ~ 3%. Second, fast neutrons with momenta greater than ~ 14 GeV/c will fall within the accepted timing window. A priori, since the energy of the electron beam is only 16 GeV/c, one would not expect the number of such neutrons to be large. In fact, using an extrapolation of the momentum distributions given by Brody, et al.,[8] the admixture of fast neutrons is expected to be only about 1%. The total admixture however can be estimated from the date of the present experiment itself, from a comparison of the cross sections observed with and without the aluminum absorber inserted. If, for example, the neutron admixture were zero, then one would not expect to see any significant change in the measured cross section when the aluminum absorber is withdrawn. The estimate can be made as follows:

The ratio R of the observed to the true K_L^0 cross section can be written in terms of the neutron cross section and the detected neutron/kaon intensity ratio X, with the aluminum absorber inserted, according to the equation

$$R = 1 + \frac{1}{a_K} \ln\left(\frac{1 + X}{1 + Xe^{-(a_n - a_K)}}\right) \qquad (1)$$

where a_K and a_n are the target thickness expressed in K_L^o and neutron interaction lengths, respectively. We can then write the following equation for X,

$$X = \frac{e^{a_K(R-1)}}{1 - e^{(a_K R - a_n)}} \qquad (2)$$

and a similar equation for X', the neutron/kaon intensity ratio with the aluminum absorber withdrawn. Since X and X' are small their values depend little on a_n but are very sensitive to a_K. The difference $\Delta X = X' - X$, however, is insensitive to a_K. Accordingly, we compute ΔX for each target and obtain an average value of $\Delta X = 0.07 \pm 0.04$. Moreover, we know that the effect of the aluminum absorber should be to attenuate the neutron flux relative to the kaon flux by a factor which depends upon the relative cross sections and the absorber length. The precise absorber length is unknown, since it consisted in part of a complex aluminum frame, and is best inferred from its effect on the observed rate at flight times either shorter than 1.9 nS or longer than 9.0 nS. We choose the latter since this result should be insensitive to fluctuations in the timing resolution. In this way, using as first estimates of the K_L^o and neutron cross sections the values observed at short and long flight times respectively, we find that the effect of the aluminum absorber should be to attenuate the neutron flux by a factor of 1.42 relative to the kaon flux, i.e., $X' = 1.42\,X$.

From these two relations we conclude that $X = 0.17 \pm 0.09$ Similarly, if we repeat this calculation using the apparent cross sections in the flight time intervals 1.0 - 1.9 nS and 1.9 - 3.0 nS, we obtain values of $X = 0.01 \pm 0.09$ and 0.60 ± 0.17, respectively. These results suggest that, with the aluminum absorber inserted, significant numbers of neutrons are present only for flight times longer than about 1.8 nS. The mean value of X for flight times shorter than 1.8 nS, after subtracting the slow neutron admixture, is $X = 0.06 \pm 0.06$, and we use this number as our best estimate of the fast neutron admixture for flight times less than 1.0 nS. The observed K_L^0 cross sections given in Table 1 are taken solely from the data with the aluminum absorber inserted. They are corrected only for a 3% admixture of slow neutrons. The statistical and systematic errors are shown separately, the latter reflecting a possible 6% admixture of fast neutrons. No significant correction is necessary for the small amount ($\leq 0.5\%$) of diffraction scattering accepted by the detector.

Next we consider the neutron total cross sections which can be obtained from the data in the flight time intervals 9-12 nS and 12-18 nS. These intervals correspond, respectively, to neutron momenta in the ranges 4.2 - 4.8 GeV/c and 3.4 - 4.2 GeV/c. The observed cross sections are included in Fig. 2. From these data there is no significant evidence for a change in the measured cross section either with flight time or beam condition. The survey information of Brody, et al., suggests that the kaon admixture in these timing intervals should be ~ 10%. It can, however, be larger or smaller, depending upon the variation with flight time of the relative efficiency for the detection of kaons and neutrons.

We conclude that the error introduced into the cross section by a possible kaon admixture is negligible in comparison to the quoted statistical error. We therefore combine all the data in the flight time interval 9 - 18 nS for both beam conditions in arriving at the neutron cross sections given in Table 2. In principle, a correction is also necessary for the admixture of antineutrons in the beam. The yield of antiprotons relative to protons has been measured at SLAC,[9] and in the range 3.4 - 4.8 GeV/c is approximately 3%. Using the optical model and the elementary antiproton cross sections, we find that a 3% admixture of antineutrons should induce a change of only 0.6% in the measured neutron cross sections. This correction is small in comparison to the measured statistical errors, and has not been applied to the cross sections given in Table 2.

Finally, we compare the cross sections observed in the present experiment with those computed from the optical model and, where possible, with the results of previous experiments. According to the optical model, in the high energy approximation, the K_L^o total cross section is determined by the forward scattering amplitudes of the elementary K^o and $\bar{K}^o$ -nucleon interactions and by the spatial extent of the nuclear potential. The cross sections predicted by the optical model are shown in Table 1. The elementary K^o and $\bar{K}^o$ cross sections were obtained using charge independence, from published K^+ and K^- - nucleon cross sections,[10] and ratios of real to imaginary parts of the forward scattering amplitudes were taken from dispersion relation calculations.[11] The nuclear potential was assumed to follow the charge distributions found in electron scattering experiments.[12] The errors attached to the computed cross sections are determined by the errors in the elementary cross sections and in the ratios of the real to the imaginary parts of the elementary amplitudes. Within the accuracy of the present experiment and the uncertainty in the optical model calculation, the measured K_L^o cross sections are in agreement with the predictions of the optical model.

Figure 3 shows previous measurements of neutron-nucleus total cross sections together with those deduced from the present experiment as a function of neutron momentum. Also in this figure we show the cross sections computed from the optical model. In this calculation the elementary neutron-nucleon cross sections were taken from the measurements of Bugg, et al.,[13] and ratios of real to imaginary parts of forward scattering amplitudes from dispersion relation calculations.[14] The nuclear potentials used are the same as those previously described for the K_L^o calculation. The optical model results are also shown in Table 2. The indicated errors derive from present uncertainties in the elementary scattering amplitudes. The results of the present experiment are in good agreement with the cross sections calculated from the optical model, as are the previous measurements at 2.1, 5.7 and 10 GeV/c.

ACKNOWLEDGEMENTS

We are indebted to Professor O. Kofoed-Hansen of CERN for discussions on the optical model calculation, to the staffs of the Stanford Linear Accelerator Center and the High Energy Physics Laboratory, in particular Mr. F. T. Halbo, Mr. R. L. Parks, Mr. L. G. Doster, and Mr. R. P. Hermann, for their cooperation throughout the running of this experiment and to

Professor R. Hofstadter, Director of the High Energy Physics Laboratory, for his interest in and support of this work.

TABLE 2

Target	Total cross sections (mb)	
	Observed	Predicted
Carbon	369 ± 7	349 ± 5
Aluminum	666 ± 16	678 ± 9
Copper	1331 ± 17	1357 ± 17
Lead	3071 ± 79	3118 ± 33

A comparison between the observed and calculated neutron-nucleus total cross sections. The average neutron momentum is 3.8 GeV/c.

REFERENCES

* Work supported in part by the U. S. Office of Naval Research Contract [Nonr 225 (67)] and the National Science Foundation Grant GP-9498.

† Now at the Stanford Linear Accelerator Center, Stanford University, Stanford, California.

‡ National Science Foundation Predoctoral Fellow.

§ National Science Foundation Senior Postdoctoral Fellow on leave from Johns Hopkins University.

1) R. J. Glauber, Lectures in Theoretical Physics, edited by W. E. Brittin and L. G. Dunham (Interscience Publishers, Inc., New York, 1959), Vol. 1, p. 315.

2) T. Coor, D. A. Hill, W. F. Hornyak, L. W. Smith and G. Snow, Phys. Rev. 98, (1955) 1369.

3) J. H. Atkinson, W. N. Hess, V. Perez-Mendez and R. Wallace, Phys. Rev. 123 (1961) 1850.

4) V. S. Pantuev and M. N. Khachaturyan, JETP Lett. 15 (1962) 626.

5) J. Engler, K. Horn, J. König, F. Mönning, P. Schludecker, H. Schopper, P. Sievers, H. Ullrich and K. Runge, Phys. Letts. 28B (1964) 64.

6) L. W. Jones, M. J. Longo, J. R. O'Fallon, M. N. Kreisler, Phys. Letts. 27B (1968) 328.

7) E. F. Parker, T. Dobrowolski, H. R. Gustafson, L. W. Jones, M. J. Longo, F. E. Ringia, and B. Cork, Phys. Letts. 31B (1970) 250.

8) A. D. Brody, W. B. Johnson, D.W.G.S. Leith, G. Loew, J.S. Loos, G. Luste, R. Miller, K. Moriyasu, B.C. Shen, W.M. Smart and R. Yamartino, Phys. Rev. Letts. 22, (1969) 966.

9) S.M. Flatté, M. Peters, P. R. Klein, L.H. Johnston, and S.G. Wojcicki, Phys. Letts. 18 (1967) 366.

10) W. Galbraith, E.W. Jenkins, T.F. Kycia, B.A. Leontic, R.H. Phillips A.L. Read and R. Rubinstein, Phys. Rev. 138 (1965) B913.

11) M. Lusignoli, M. Restignoli, G. Violini, and G.A. Snow, Nuovo Cimento XLV (1966) A792 and IL (1967) A705.

12) For carbon we use a modified harmonic oscillator potential

$$\rho \propto \left(1 + \frac{r^2}{B^2}\right) \exp \frac{-r^2}{A^2}$$

with $A = 1.65$ F and $B = 1.71$ F, taken from recent unpublished work at our laboratory by I. Sick and J.S. McCarthy. For aluminum and copper we use a Woods-Saxon potential

$$\rho \propto \left(1 + \exp \frac{r - c}{z}\right)^{-1}$$

with $(c,z) = (3.09$ F, 0.50 F$)$ and $(4.30$ F, 0.57 F$)$ for aluminum and copper respectively. For lead we use a modified gaussian potential

$$\rho \propto \left(1 + w \frac{r^2}{c^2}\right) \left(1 + \exp \left(\frac{r^2 - c^2}{z^2}\right)\right)^{-1}$$

with $c = 6.30$ F, $z = 2.89$ F, and $w = 0.34$, taken from J. Heisenberg, R. Hofstadter, J.S. McCarthy, I. Sick, B.C. Clark, R. Herman and D.G. Ravenhall, Phys Rev. Letts. 23 (1969) 1402.

13) D.V. Bugg, D.C. Salter, G.H. Stafford, R.F. George, K.F. Riley and R.J. Tapper, Phys. Rev. 146 (1966) 980.

14) P. Söding, Phys. Rev. Letts. 8 (1964) 285; and A.A. Carter and D.V. Bugg, Phys. Letts. 20 (1966) 203.

FIGURE CAPTIONS

Fig. 1. A schematic drawing of the K^0 detector.

Fig. 2. The measured total cross sections versus flight time for the two beam conditions.

Fig. 3. A summary of existing measurements of neutron-nucleus total cross sections versus neutron momentum. Measurements have been made on certain other nuclei but for clarity are not shown. The solid lines show the results of the optical model calculation.

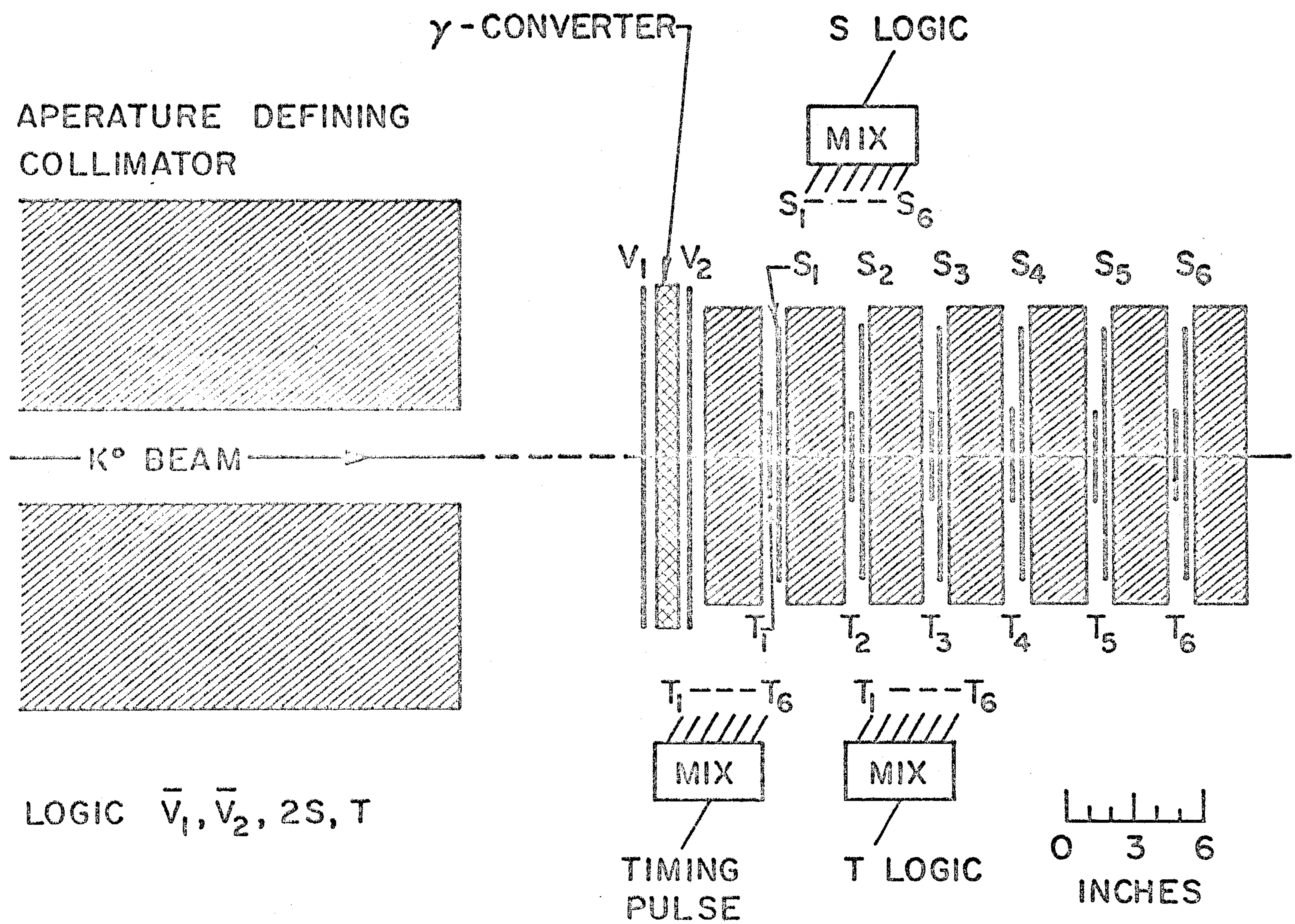
γ-CONVERTER
S LOGIC
APERATURE DEFINING
COLLIMATOR
MIX
S_1 - - - S_6
V_1
V_2
S_1
S_2
S_3
S_4
S_5
S_6
K° BEAM
T_1
T_2
T_3
T_4
T_5
T_6
T_1 - - - T_6
MIX
T_1 - - - T_6
MIX
LOGIC $\bar{V}_1, \bar{V}_2, 2S, T$
TIMING
PULSE
T LOGIC
0 3 6
INCHES

FIGURE 1

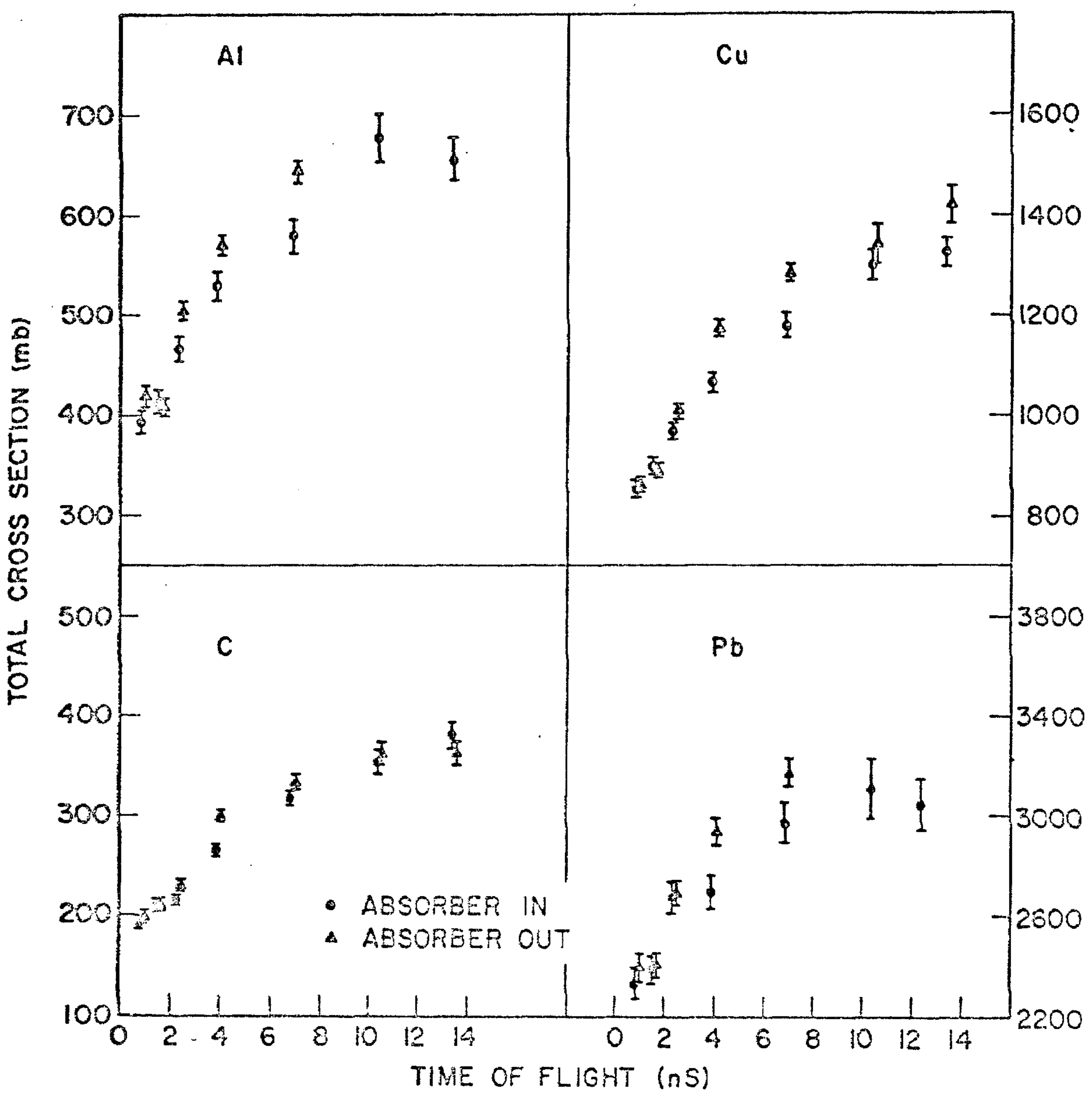
Al
Cu
C
Pb
TOTAL CROSS SECTION (mb)
TIME OF FLIGHT (nS)
ABSORBER IN
ABSORBER OUT
700
600
500
400
300
200
100
1600
1400
1200
1000
800
3800
3400
3000
2600
2200
0
2
4
6
8
10
12
14

FIGURE 2

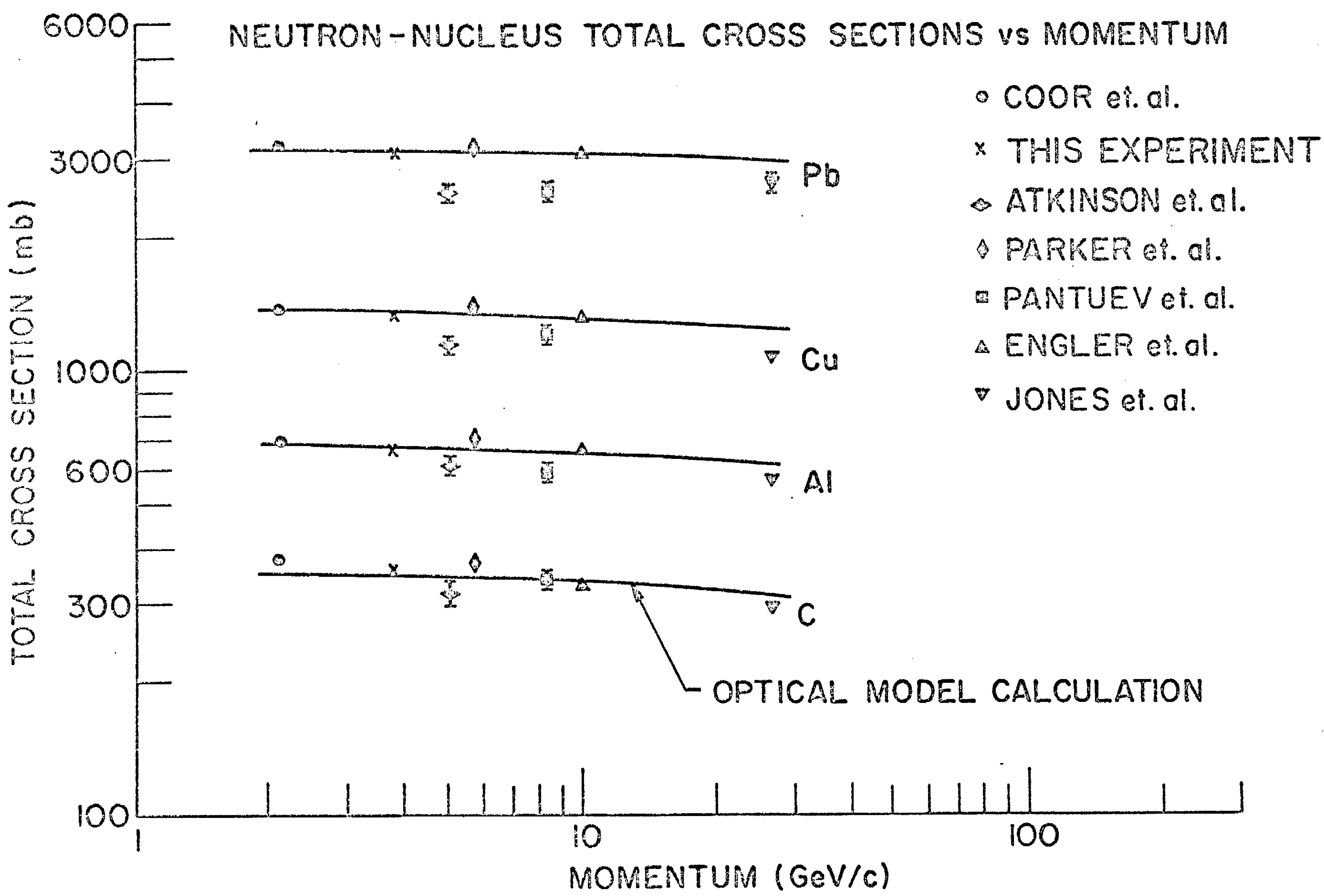
NEUTRON-NUCLEUS TOTAL CROSS SECTIONS vs MOMENTUM
COOR et. al.
THIS EXPERIMENT
ATKINSON et. al.
PARKER et. al.
PANTUEV et. al.
ENGLER et. al.
JONES et. al.
Pb
Cu
Al
C
OPTICAL MODEL CALCULATION
TOTAL CROSS SECTION (mb)
6000
3000
1000
600
300
100
1
10
100
MOMENTUM (GeV/c)

FIGURE 3